ESTIMATION OF MORTAR BRICK COMPOSITION FROM SPECTRAL REFLECTANCE

Zakaria Bnoulkacem[1] Bikram Koirala[1], Philippe Soubrier[2],
Xueqing Hu[2], Michiel Vlaminck[3], Hiep Luong[3], Nathan Van Den Bossche[2], Paul Scheunders[1]

[1] Imec-Visionlab, University of Antwerp (CDE) Universiteitsplein 1, B-2610 Antwerp,
[2] Building Physics Research Group, Ghent University, Belgium,
[3] IPI-URC-imec, Ghent University, Belgium

ABSTRACT

Characterization of mortar samples from spectral reflectance is essential for both the conservation of historical buildings and modern construction practices. We propose an approach to estimate the composition of mortar by spectral unmixing. Changes in the spectral reflectance of raw powder mixtures after chemical reactions with water complicate the problem. The challenge becomes even more pronounced when the endmember spectra of the cured pure components are unavailable for unmixing. The proposed approach mitigates spectral variability by projecting the dataset onto the unit hypersphere on which the endmembers are estimated using a minimum volume optimization technique. The endmembers are then manually assigned to the pure components and the original composition of the mortar samples is determined by minimizing the reconstruction error between the measured and reconstructed spectra. The methodology was validated using spectral reflectance data from 93 different mortar samples. Experimental results demonstrate the potential of the proposed approach.

***Index Terms*—** Hyperspectral imaging, Mortar characterization, Spectral unmixing, Cultural heritage conservation, Construction materials

1. INTRODUCTION

Mortar is a crucial component of nearly all structures. Its ubiquity makes a rapid and accurate non-destructive estimation of its composition essential for both the conservation and anastylosis efforts of current and historical buildings. Likewise, the accurate estimation of mortar component composition allows for the deduction of its physical properties and the matching of historical materials used, leading to preserved authenticity and avoiding damage to historical buildings and important architectural pieces [1]. Consequently, there exists a need for reliable methods for mortar component characterization and estimation [2].

Recently, hyperspectral image analysis techniques have been increasingly used in the context of mortar materials, either for categorizing different types of mortar samples or to estimate their compositions or physical properties [3, 4, 5, 6, 7, 8]. To estimate the composition of mortar samples, hyperspectral unmixing approaches may come in handy, but have not yet been explored in this context.

The main purpose of hyperspectral unmixing is to determine the proportion of pure material spectra, known as endmembers, present within each pixel. This is typically done by reducing the discrepancy between the measured spectral reflectance and the spectrum predicted by a chosen mixing model. Although advanced hyperspectral unmixing methods are constantly being developed, many of these methods struggle when the acquired datasets are affected by spectral variability [9]. This variability often arises from changes in illumination and acquisition conditions. The challenge is further compounded when no spectra of pure material are present in the dataset. Although several recent approaches have attempted to simultaneously estimate endmembers and fractional abundances [10], [11], they still fall short in effectively handling spectral variability.

The main goal of this work is to estimate the original composition of mortar samples, i.e., the fractional abundances of the original raw powders that have been used to create the samples. A major challenge is the significant difference between the spectral reflectance of raw powder mixtures and that of cured samples. This discrepancy is partly due to the fact that the raw powders undergo chemical reactions with water, forming complex compounds. An additional challenge is that no pure endmember spectra are available in the reflectance data of the cured mortar samples. The raw powders are not suitable, and even if one had access to cured pure component samples, their spectral reflectance may not be suitable either, due to the complex chemical reactions in the mixtures. To reliably estimate the composition of cured samples (fractional abundances), we developed an effective unmixing method that can estimate the endmembers, relate them to the original raw components, and estimate the corresponding abundances.

2. DATASET AND METHODOLOGY

2.1. Dataset

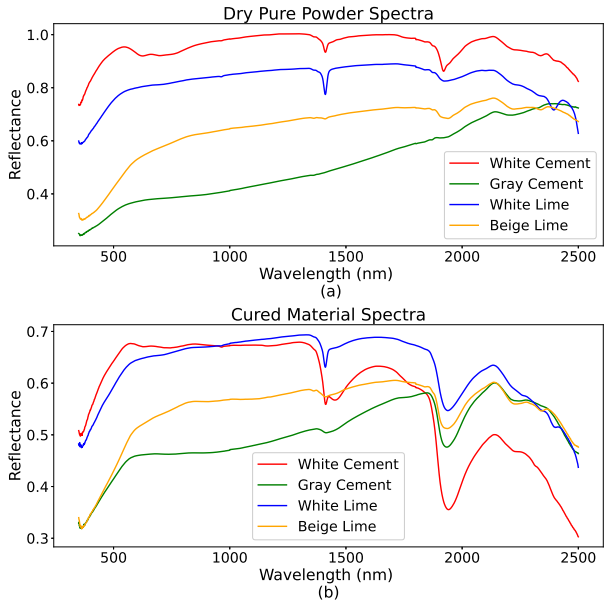

Fig. 1. plot of the spectra of pure dry powders and the cured pure bricks.

In this work, we prepared a total of 93 mixtures using four pure mineral powders commonly used as binder agents in both historic and modern construction materials: gray cement, white cement, beige lime, and white lime. gray and white cements primarily consist of Portland cement and limestone, whereas white lime and beige lime are mainly composed of calcium carbonate and silica. Of these mixtures, 41 are binary (containing two components), 41 are ternary (three components), and the remaining 11 are quaternary (all four components). The total mass of each mixture is approximately 211 g. Each of these mixtures was then supplemented with 500 g of sand, followed by the addition of sufficient water (approximately 90 g) to ensure the mixture was pourable and suitable for proper curing. The prepared mixtures were then poured into moulds and allowed to fully cure and dry completely. These fully cured samples are referred to as mortar bricks (see Fig. 2 for the corresponding RGB image). In addition to the 93 samples, four additional samples were prepared by mixing each of the four original mineral powders with sand and water. These are referred to as pure mortar bricks.

The spectral reflectances of mortar bricks, pure mortar bricks, and pure mineral powders were then measured under laboratory conditions using an ASD spectroradiometer. The data from the spectroradiometer has 2151 spectral bands, ranging from 350 to 2500 nm with a step size of 1 nm. Fig. 1 shows the spectral reflectances of the pure mineral powders along with the pure mortar bricks. As expected, the spectral reflectance of the cured pure mortar bricks differs significantly from that of the pure mineral powders. The pure mineral powders (see Fig. 1 (a)) have spectral features around 1400 nm and 1900 nm, indicating the presence of vibrational hydroxyl processes [12]. On the other hand, the spectral features of the cured pure mortar bricks in these wavelength ranges are enhanced and distorted, due to the formation of new compounds such as Calcium Silicate Hydrate [13]. Moreover, due to carbonation during or after the curing process, the spectra of the cured pure mortar bricks may be influenced by the presence of calcium carbonate, particularly around 2300 and 2500 nm. Because the effects of calcium carbonate and calcium silicate hydrate may hinder the composition estimation, we decided to remove the wavelengths above 1700 nm from the spectra. Additionally, because the sample color strongly influences the signal in the visible and near-infrared range (350–1000 nm), and this same wavelength range lacks distinctive absorption features (see Figure 1), it was also removed. Therefore, the spectra were truncated to the 1100–1700 nm range for further analysis.

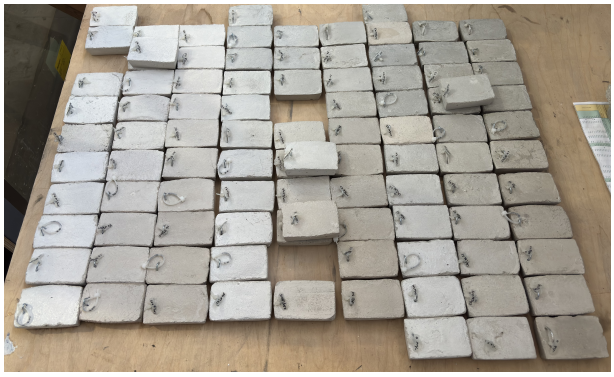

Fig. 2. RGB image of the 97 mortar bricks.

2.2. Methodology

The required unmixing procedure should estimate both endmembers and fractional abundances. Endmembers are estimated by a minimum volume optimization of the data manifold, which requires a data simplex whose faces pass through the spectral reflectances of the binary mixtures. Moreover, variations in illumination and acquisition conditions must be addressed. In general, the proposed method consists of three main steps: (a) tackling spectral variability; (b) estimating endmembers; and (c) estimating the fractional abundances.

2.2.1. Tackling spectral variability

Scaling effects induced by variation in illumination and acquisition conditions can be tackled by projecting each measured

spectrum onto the unit hypersphere:

$$\mathbf{y} \rightarrow \frac{\mathbf{y}}{\|\mathbf{y}\|} \tag{1}$$

where the function $||\cdot||$ denotes the Euclidean norm, which computes the length (magnitude) of the vector.

2.2.2. *Estimating endmembers*

As demonstrated in [11], to accurately estimate the endmembers of a dataset, at least one binary mixture should be present on each face of the data simplex. If this condition is met, the endmembers and abundances can be simultaneously estimated by optimizing the following equation:

$$\hat{\mathbf{E}}, \hat{\mathbf{A}} = \arg\min_{\mathbf{E},\mathbf{A}} \frac{1}{2}||\mathbf{Y} - \mathbf{E}\mathbf{A}||_F^2 + \lambda \left\|\mathbf{E} - \mathbf{m}\mathbf{1}_p^T\right\|_F^2$$
$$\text{s.t.} 0 \leq \mathbf{E} \leq 1, 0 \leq \mathbf{A} \leq 1, \mathbf{1}^T\mathbf{A} = \mathbf{1_N} \tag{2}$$

where p denotes number of endmembers, $\mathbf{E} = [\mathbf{e_1}, \mathbf{e_2}, \cdots, \mathbf{e_p}]$ is the endmember matrix, $\mathbf{Y} = [\mathbf{y_1}, \mathbf{y_2}, \cdots, \mathbf{y}_N]$ represents the measured spectra, $\mathbf{A} = [\mathbf{a_1}, \mathbf{a_2}, \cdots, \mathbf{a}_N]$ is the matrix containing the compositions of the N mixtures, λ is a regularization parameter, and $\mathbf{m}$ is a vector that contains the mean values of the spectral pixels.

Each estimated endmember is then assigned to one of the pure components by visually comparison with the spectra of both pure powders and cured mortar bricks.

2.2.3. *Estimating the fractional abundances*

To improve the estimated fractional abundances, in the final step, for each pixel we optimize the following equation:

$$\left|\left|\frac{\mathbf{y}}{||\mathbf{y}||} - \frac{\mathbf{E}\mathbf{a}}{||\mathbf{E}\mathbf{a}||}\right|\right|_2^2, \text{s.t.} \mathbf{a} \geq 0, \mathbf{1}^T\mathbf{a} = \mathbf{1} \tag{3}$$

We would like to clarify that while Eq. (2) optimizes the reconstruction error for the spectral reflectance of all mixtures simultaneously, Eq. (3) does this for each single mixture separately.

3. RESULTS AND DISCUSSION

We applied the proposed approach to the spectral reflectance data of the mortar bricks acquired with the ASD spectroradiometer (see Section 2). In the first step, all measured spectra were projected onto the unit hypersphere. By utilizing the entire dataset of cured mortar samples, the endmembers were estimated in the subsequent step by optimizing Eq. (2). The estimated endmembers are shown in Fig. 3. For comparison, the spectra of the dry pure minerals and the cured pure mortar bricks are also presented. One can observe that the endmembers estimated using the proposed approach show a high degree of similarity to the spectra of the cured pure mortar bricks.

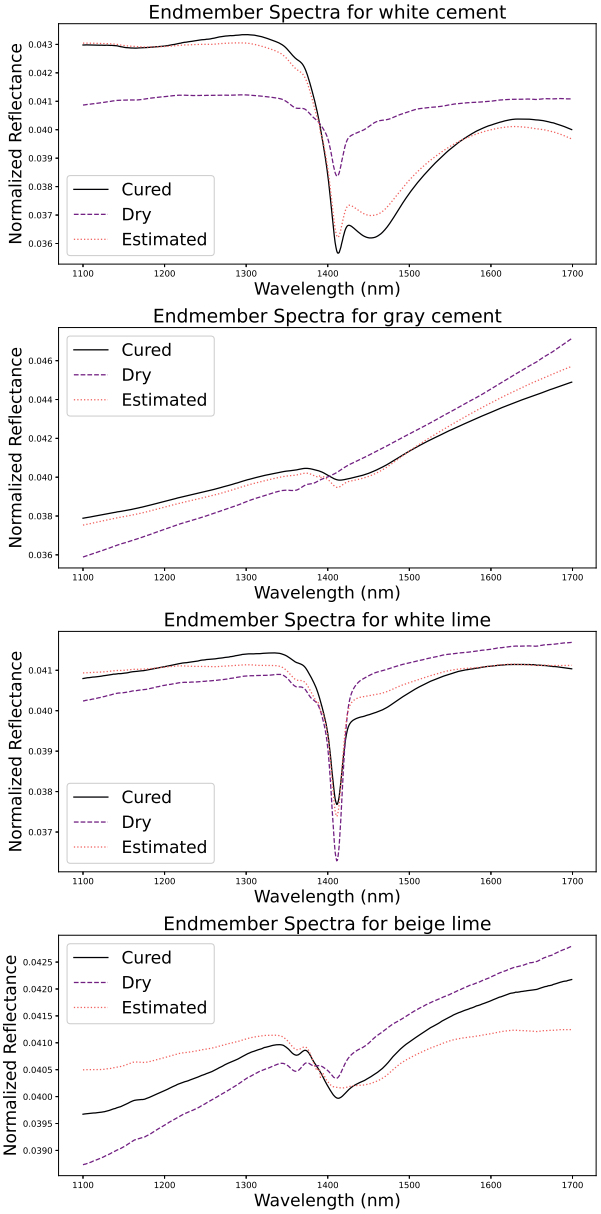

Fig. 3. Dry, cured, and estimated endmember spectra.

To further quantify the results, Table 1 reports the spectral angle distance (SAD) between the estimated and measured spectral reflectances:

$$\text{SAD(x,y)} = \text{acos}\left(\frac{\mathbf{x}^T\mathbf{y}}{\|\mathbf{x}\|\,\|\mathbf{y}\|}\right) \times 180/\pi \tag{4}$$

As can be observed, the average SAD values between the estimated spectra and the measured spectra of the pure mortar bricks are relatively low, indicating good agreement. In contrast, the measured spectra from the dry powders show sig-

Material	Dry vs Cured	Dry vs Estimated	Cured vs Estimated
White Cement	2.8967°	2.6162°	0.4567°
Gray Cement	1.7960°	1.4243°	0.4914°
White Lime	0.8267°	0.6628°	0.2870°
Beige Lime	0.7743°	1.5036°	0.7657°
Average SAD Values			
Average	**1.5734°**	**1.5517°**	**0.5002°**

Table 1. SAD values between estimated endmembers, dry pure powders, and the cured spectra of pure mortar bricks.

nificant deviations from the estimated ones and those of the cured samples, particularly in the case of white cement.

In the final step, we estimated the fractional abundances of each mixture by using the endmembers obtained in the previous step and optimising Eq. (3). The Abundance root mean squared error (RMSE):

$$\text{Abundance RMSE} = \sqrt{\frac{1}{pN}\sum_{j=1}^{p}\sum_{i=1}^{N}\left(\hat{\mathbf{A}}_{ij} - \mathbf{A}_{ij}\right)^2} \quad (5)$$

between the estimated and ground truth values is reported in Table 2. For comparison, the fractional abundances estimated using the spectra of the pure mineral powders and the pure mortar bricks as endmembers are also presented.

Material	Dry Endmembers	Cured Endmembers	Estimated Endmembers
White Cement	0.5914	0.1974	0.2154
Gray Cement	0.1387	0.1719	0.1433
White Lime	0.3707	0.2335	0.2190
Beige Lime	0.3212	0.2093	0.1597
Average abundance RMSE Values			
Average	**0.3555**	**0.2030**	**0.1844**

Table 2. Abundance RMSE values between the ground truth fractional abundances and the estimated ones using dry, cured, and estimated endmember spectra.

As expected, using the spectra of pure mineral powders as endmembers resulted in a high RMSE, particularly for white cement and white lime. For these materials, the spectral distortion is more pronounced (see Fig. 3). The use of the estimated endmembers yielded slightly better results compared to those obtained using spectra from the pure mortar bricks.

Another approach to quantitatively assess the performance of the proposed methodology is to compute the reconstruction error between the measured and estimated reflectance values. However, in this work, we opted to visualise the reconstruction quality by overlaying the PCA projection of the reconstructed dataset on that of the measured data. As shown in Fig. 4, the data points reconstructed using the proposed method lie close to the true ones. In contrast, the reconstructions based on spectra from pure mortar bricks as endmembers exhibit a slight shift, while the worst performance is observed when pure mineral powders are used for the reconstruction.

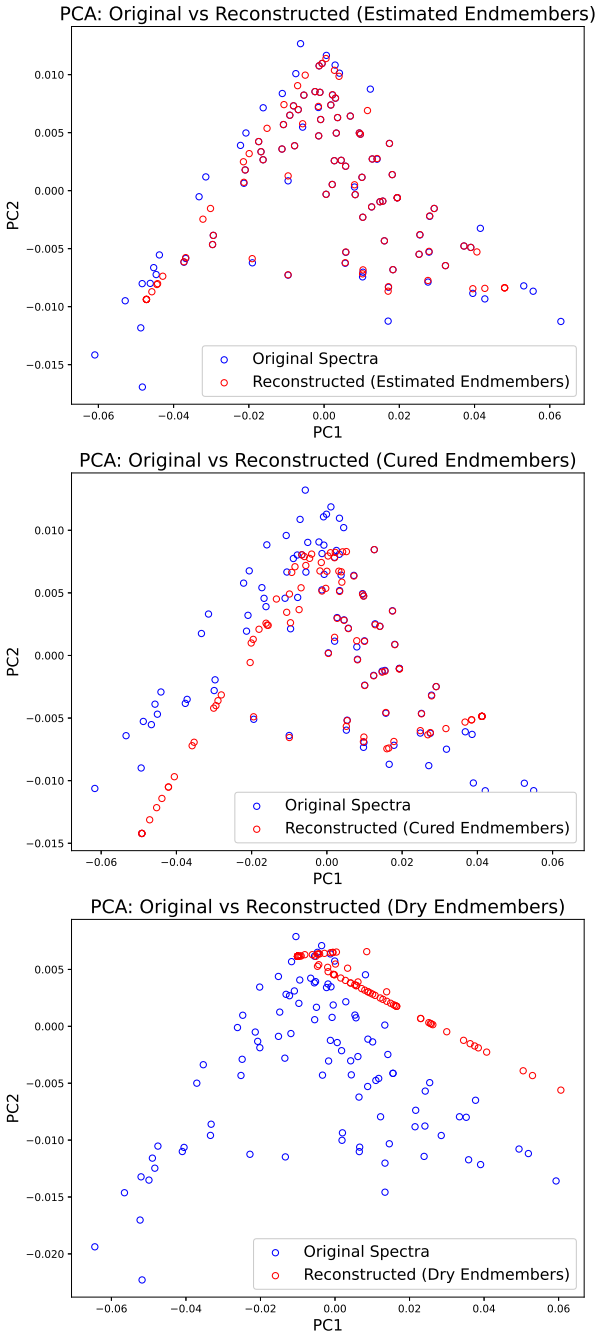

Fig. 4. PCA plot of measured spectra and reconstructed spectra using dry, cured, and estimated endmembers.

4. CONCLUSION

In this work, we developed an effective unmixing method capable of estimating the endmember spectra of mortar bricks, relating them to raw components, and estimating their composition. The methodology was validated on a dataset generated under controlled laboratory conditions, containing cured

mortar bricks of mixtures of 4 pure powder component with a fixed amount of sand and water. The estimated endmembers differed from the spectra of the pure powders but closely resembled the measured spectra of the cured pure mortar bricks (containing one of the pure powders, sand, and water). Moreover, they yielded slightly better abundance estimations compared to those obtained from the pure mortar bricks. These results show the potential of the proposed approach for practical on-site applications of mortar composition estimations, where no pure mortar samples are available.

5. ACKNOWLEDGMENT

The research presented in this paper is funded by the Research Foundation-Flanders (project G031921N). Zakaria Bnoulkacem is a doctoral fellow of the Research Foundation Flanders, Belgium: FWO grant number : 1SH1M24N. Bikram Koirala is a postdoctoral fellow of the Research Foundation Flanders, Belgium (FWO: 1250824N-7028)

6. REFERENCES

[1] Selvaraj Thirumalini, Ramadoss Ravi, and Murugan Rajesh, "Experimental investigation on physical and mechanical properties of lime mortar: Effect of organic addition," *Journal of Cultural Heritage*, vol. 31, pp. 97–104, 2018.

[2] Maphole Loke, Kumar Pallav, and Giuseppe Cultrone, "Challenges in characterization and development of suitable historic repair mortars," *International Journal of Conservation Science*, vol. 14, pp. 783–802, 09 2023.

[3] Bikram Koirala, Zohreh Zahiri, Mahdi Khodadadzadeh, and Paul Scheunders, "Fractional abundance estimation of mixed and compound materials by hyperspectral imaging," in *2019 10th Workshop on Hyperspectral Imaging and Signal Processing: Evolution in Remote Sensing (WHISPERS)*, 2019, pp. 1–5.

[4] Liang Fan, Ming Fan, Abdullah Alhaj, Genda Chen, and Hongyan Ma, "Hyperspectral imaging features for mortar classification and compressive strength assessment," *Construction and Building Materials*, vol. 251, pp. 118935, 2020.

[5] Love Eriksson, *Hyperspektral bildanalys av murbruk från Carcassonnes inre stadsmurar : En studie om applikationen av nära infraröd spektroskopi som en ickedestruktiv metod för klassificering av historiskt murbruk*, Ph.D. thesis, Umeå University, Department of historical, philosophical and religious studies, 2018.

[6] Genda Chen, Hongyan Ma, Pengfei Ma, Liang Fan, and Abdullah Alhaj, "Hyperspectral imaging analysis for mechanical and chemical properties of concrete and steel surfaces," Tech. Rep., Missouri University of Science and Technology, 2023.

[7] Zohreh Zahiri, Debra F. Laefer, and Aoife Gowen, "Classification of hardened cement and lime mortar using short-wave infrared spectrometry data," in *Structural Analysis of Historical Constructions*, Rafael Aguilar, Daniel Torrealva, Susana Moreira, Miguel A. Pando, and Luis F. Ramos, Eds., Cham, 2019, pp. 437–446, Springer International Publishing.

[8] Soubrier, Philippe and Vlaminck, Michiel and Luong, Hiep and Van Den Bossche, Nathan, "Multispectral Pathology Detection for Conservation of Heritage Buildings: A Mortar Case Study," in *4th International Conference TMM-CH: Transdisciplinary Multispectral Modelling and Cooperation for the Preservation ofCultural Heritage*, 2025.

[9] Bikram Koirala, Zohreh Zahiri, Alfredo Lamberti, and Paul Scheunders, "Robust supervised method for nonlinear spectral unmixing accounting for endmember variability," *IEEE Transactions on Geoscience and Remote Sensing*, vol. 59, no. 9, pp. 7434–7448, 2021.

[10] Behnood Rasti, Bikram Koirala, and Paul Scheunders, "Hapkecnn: Blind nonlinear unmixing for intimate mixtures using hapke model and convolutional neural network," *IEEE Transactions on Geoscience and Remote Sensing*, vol. 60, pp. 1–15, 2022.

[11] Behnood Rasti, Bikram Koirala, Paul Scheunders, and Jocelyn Chanussot, "Misicnet: Minimum simplex convolutional network for deep hyperspectral unmixing," *IEEE Transactions on Geoscience and Remote Sensing*, vol. 60, pp. 1–15, 2022.

[12] Etienne Ducasse, Karine Adeline, Xavier Briottet, Audrey Hohmann, Anne Bourguignon, and Gilles Grandjean, "Montmorillonite estimation in clay–quartz–calcite samples from laboratory swir imaging spectroscopy: A comparative study of spectral preprocessings and unmixing methods," *Remote Sensing*, vol. 12, no. 11, 2020.

[13] Ping Yu, R. James Kirkpatrick, Brent Poe, Paul F. McMillan, and Xiandong Cong, "Structure of calcium silicate hydrate (c-s-h): Near-, mid-, and far-infrared spectroscopy," *Journal of the American Ceramic Society*, vol. 82, no. 3, pp. 742–748, 1999.